https://doi.org/10.5194/wes-2019-28
Preprint. Discussion started: 8 July 2019
© Author(s) 2019. CC BY 4.0 License.

eawe european academy of wind energy
Open Access WIND ENERGY SCIENCE DISCUSSIONS

Optimal relationship between power and design driving loads for wind turbine rotors using 1D models

Kenneth Loenbaek[1,2], Christian Bak[2], Jens I. Madsen[1], and Bjarke Dam[1]

[1]Suzlon Blade Science Center, Havneparken 1, 7100 Vejle, Denmark
[2]Technical University of Denmark, Frederiksborgvej 399, 4000 Roskilde, Denmark

Correspondence: Kenneth Loenbaek (kenneth.loenbaek@suzlon.com)

Abstract. We investigate the optimal relationship between the aerodynamic power, thrust loading, and size of a wind turbine rotor when its design is constrained by a static aerodynamic load. Based on 1D-axial momentum theory, the captured power $\tilde{P}$ for a uniformly loaded rotor can be expressed in terms of the rotor radius R and the rotor thrust coefficient C_T. Common types of static Design Driving Load Constraints (DDLC), e.g. limits on permissible root-bending moment or tip deflection, may be generalized into a form that also depends on C_T and R. Using these relationships to maximize $\tilde{P}$ subject to a DDLC, shows that operating the rotor at the Betz limit (maximum C_P) does not lead to the highest power capture. Rather, it is possible to improve performance with a larger rotor radius and lower C_T without violating the DDLC. As an example, a rotor design driven by a tip-deflection constraints, may achieve 1.9% extra power capture $\tilde{P}$ compared to the baseline (Betz limit) rotor.

The method is extended for optimization of rotors with respect to Annual Energy Production (AEP), where the thrust characteristics $C_T(V)$ needs to be determined together with R. This results in much higher relative potential for improvements, since the constraint limit can be met over a larger range of wind speeds. For example, a relative gain in AEP of $+5.7\%$ is possible for a rotor design constrained by tip deflections compared with a rotor designed for optimal C_P. The optimal solution for AEP leads to a thrust curve with three distinct operational regimes and so called thrust-clipping.

Keyword: Wind Energy, Wind Turbine, Initial rotor design, Low Induction Rotor, Thrust-clipping, Peak-shaving

1 Introduction

Since the start of the wind energy industry it has been a clear trend that the rotor size is increasing. But as it has been discussed in Sieros et al. (2012) the increasing rotor size is not a clear way to decrease the Cost of Energy (CoE), since the weight (which is closely related to cost) of the rotor always will scale with a higher exponent than the increase in power. It is therefore argued that the lower CoE, that has taken place, is mostly due to technology improvements. The structural design of the turbine is built to carry the loads coming from the aerodynamics (steady or extreme) and the self weight. Therefore lowering the loads should lead to a lighter blade. The steady aerodynamic load is applied in order to extract power and increasing the load leads to a higher power until maximum power efficiency (max C_P) is reached. Increasing the load should lead to a heavier blade but it also leads to a higher power production. It goes to show that understanding the relationship between loading, power production and structural response is very important to get the most cost effective turbine. It follows a trend that has been in the recent year

https://doi.org/10.5194/wes-2019-28
Preprint. Discussion started: 8 July 2019
© Author(s) 2019. CC BY 4.0 License.

eawe european academy of wind energy
Open Access WIND ENERGY SCIENCE DISCUSSIONS

that wind turbine optimization should include a more holistic approach with concepts like Multidisciplinary Design Analysis and Optimization (MDAO) and System Engineering (Fleming et al., 2016; Perez-Moreno et al., 2016; Zahle et al., 2015) here all the parts of the turbine design that affect the cost should be taken into account with the overall objective of minimizing CoE. Some of these related works focus more on the relationship between rotor loading effect on power and structural response. One of the concepts that comes out of it is the so called *Low Induction Rotor* (LIR) where the velocity induction at the rotor plane is lower than the value that maximizes the power efficiency. The concept was introduced by Chaviaropoulos and Sieros (2014) where it comes out of optimizing Annual Energy Production (AEP) by allowing the rotor to grow while constraining the flap root bending moment to be the same as a baseline. They state that the method can increase the AEP with 3.5% with a 10% increase in rotor radius hereby showing that LIR can increase AEP while keeping the same flap root bending moment. It agrees with Kelley (2017) who allowed for a change in the radial loading resulting in an AEP increase of 5% with a radius increase of 11%. It was also investigated by Bottasso et al. (2015) where they both tested the potential of using LIR for AEP improvements with load constraint as well as a cost optimized rotor. They find the same as the previous two that LIR can improve AEP, but when they consider the CoE they find the LIR is not cost effective, meaning that the additional cost of extending the blade is not compensated by the increase in power. This conclusion is opposed to the conclusion made by Buck and Garvey (2015b) where they target to minimize the ratio between Capital Expenditures (CapEx) and AEP. They arrive at LIR as the optimal solution for CapEx/AEP which is taken as a measure for CoE. Overall it seems that LIR can increase AEP while keeping the same load as a non-LIR baseline, but it is not clear if LIR is a cost effective solution.

In this paper we investigate the relationship between load, power and structural response. We will use simple analytical model like 1D-aerodynamic-momentum theory and Euler-Bernoulli-Beam theory which is rather crude approximations to use for wind turbine rotor design, but it should be understood that the result presented here is not intended to be used directly for rotor design but to show a possible way to include structural/load constraints into the design process. Instead of using a cost model we make constraints on the load/structural response relative to a baseline design and require that the load/structural response is not larger than the baseline. As it was argued above, keeping the same load does not necessary mean that the cost of the blade is the same and it is a limitation of the work. A better measure for the blade cost is to keep the mass constant, and a constraint was setup where the mass of the load carrying part of blade was kept to get a likely better constraint for an equal cost. The constraints will not include the effect from aero-elastic extreme loads as it is thought to be out of scope for an analysis at this level. But it is expected that if the extreme loads happens in normal operation there should be a relationship between the steady and extreme loads.

The paper starts by presenting the background Theory, then continues to present the Formulation of rotor design problems which leads into Results and discussion.

https://doi.org/10.5194/wes-2019-28
Preprint. Discussion started: 8 July 2019
© Author(s) 2019. CC BY 4.0 License.

eawe european academy of wind energy
Open Access WIND ENERGY SCIENCE DISCUSSIONS

2 Theory

This section will introduce the variables and the basic relationships used in this paper. It is split into two subsections: where subsection 2.1 introduces aerodynamic variables, equations, as well as the baseline rotor, while the second subsection 2.2 present scaling laws used to formulate design driving load constraints relative to the baseline rotor.

2.1 Aerodynamics

The theory for this Aerodynamics section is found in Sørensen (2016).

For wind turbine aerodynamics non-dimensional coefficients are often introduced and some of the common ones are for the rotor thrust (C_T) and power (C_P).

$$C_T = \frac{T}{\frac{1}{2}\rho V^2 \pi R^2} \tag{1}$$

$$C_P = \frac{P}{\frac{1}{2}\rho V^3 \pi R^2} \tag{2}$$

Where T and P are the rotor thrust and power respectively, ρ is the air density, V is the undisturbed flow speed and R is the rotor radius.

These definitions can be applied for any wind turbine rotor, but in this paper we will use a simplified relationship between C_T and C_P, which is derived from classical 1D-momentum theory. This implies an assumption of uniform aerodynamic loading across the rotor plane. The classical equations are often given in terms of the axial induction (a), which is defined as $a = 1 - \frac{V_{rotor}}{V}$ where V_{rotor} is the axial flow speed in the rotor plane. By combining the two classical momentum theory expressions for $C_P(a)$ and $C_T(a)$ (Sørensen, 2016, p. 11 eq. 3.8), the following relationship between these coefficients is arrived at:

$$\left.\begin{aligned} C_T(a) &= 4a(1-a) \\ C_P(a) &= 4a(1-a)^2 \end{aligned}\right\} \implies C_P(C_T) = (1-a)C_T = \frac{1}{2}\left(1+\sqrt{1-C_T}\right)C_T, \quad C_T \in [0,1[\tag{3}$$

Where $a(C_T)$ is found by inverting $C_T(a)$ and using the negative solution. A plot of C_T vs. C_P can be seen in figure 1. This $C_P(C_T)$ curve is monotonically decreasing in slope and reaches a maximum $C_P = 16/27$ corresponding to the well-known Betz-limit at $C_T = 8/9$. These monotoncity properties leads to the key observation that a reduction in thrust ($C_T = 8/9 - \Delta C_T$) will not lead to a proportional change in power (ΔC_P). This motivates this paper's investigation of the trade-off between power and load.

Power capture and Annual Energy Production (AEP)

One way to understand the power yield of a rotor is to consider equation 2 as consisting of three separate terms:

$$P = \underbrace{\frac{1}{2}\rho V^3}_{\text{Wind}} \cdot \underbrace{\pi R^2}_{\text{Size}} \cdot \underbrace{C_P}_{\text{Efficiency}} \tag{4}$$

https://doi.org/10.5194/wes-2019-28
Preprint. Discussion started: 8 July 2019
© Author(s) 2019. CC BY 4.0 License.

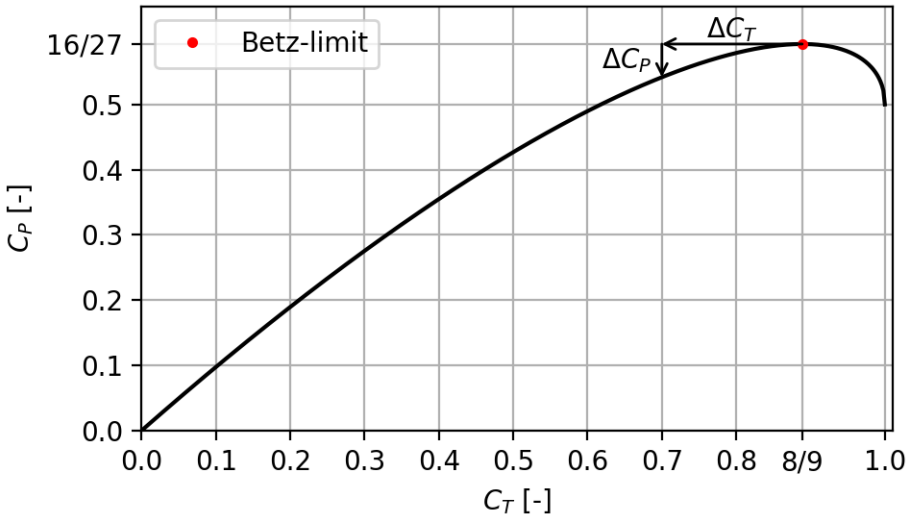

Figure 1. Relationship between normalized rotor load C_T and power efficiency C_P from one-dimensional momentum theory. Notes that around Betz-limit a small change in C_T does not lead to a proportional change in C_P, this is illustrated by ΔC_T and ΔC_P.

Wind is the part of the equation that depends on the wind conditions, *Size* is the part of the equation that depends on the rotor swept area, and *Efficiency* is how much of the potential power the rotor can extract from the kinetic power of the wind. The combination of equations 2 and 3 provides an expression that captures the latter two terms, which are the only ones affected by the design of the turbine:

$$\tilde{P}(C_T, \tilde{R}) = \frac{P}{\frac{1}{2}\rho V^3 \pi R_0^2} = C_P \tilde{R}^2 = \frac{1}{2}\left(1 + \sqrt{1 - C_T}\right) C_T \tilde{R}^2 \tag{5}$$

Where $\tilde{R}$ equals R/R_0, with R_0 being the radius of the baseline rotor. This equation will be referred to as the *Power Capture* equation. It shows that power can be changed by changing either the loading (C_T) or the rotor radius (R). This will serve as the basic equation when the power capture is optimized for a single design point.

When considering turbine design over the range of operational conditions, the *Annual Energy Production* (AEP) is introduced as an integral metric stating the energy produced per year given some wind speed frequency distribution. It can be computed as the power production (P) weighted by the probability density of wind speeds (PDF_{wind}) multiplied by the period of one year (T_{year}):

$$AEP = T_{year} \frac{1}{2} \rho \pi R_0^2 \int_{V_{CI}}^{V_{CO}} \tilde{P}(C_T(V), \tilde{R}) \cdot V^3 \cdot PDF_{wind}(V) dV \tag{6}$$

The wind speed probability distribution PDF_{wind} will be described with a Weibull distribution. V_{CI} and V_{CO} is the wind speed for *Cut In* and *Cut Out* for wind turbine operation. Here they are taken to be $V_{CI} = 3\mathrm{ms}^{-1}$ and $V_{CO} = 25\mathrm{ms}^{-1}$, which

https://doi.org/10.5194/wes-2019-28
Preprint. Discussion started: 8 July 2019
© Author(s) 2019. CC BY 4.0 License.

eawe european academy of wind energy
Open Access WIND ENERGY SCIENCE DISCUSSIONS

is common numbers for modern wind turbines.

In this paper we will use a dimensionless measure for AEP which is equivalent to the so called capacity factor, defined as follows:

$$A\tilde{E}P(C_T,\tilde{R}) = \frac{AEP}{T_{year}P_{rated}} = \frac{AEP}{T_{year}\frac{1}{2}\rho\pi R_0^2\frac{16}{27}V_0^3} = \frac{27}{16}\int_{\tilde{V}_{CI}}^{\tilde{V}_{CO}} \tilde{P}(C_T(\tilde{V}),\tilde{R})\cdot\tilde{V}^3\cdot PDF_{wind}(\tilde{V})d\tilde{V} \tag{7}$$

$\tilde{V}$ is a normalized wind speed given as $V = \tilde{V}V_0$ where V_0 is the wind speed at which the turbine reach rated power. In all of this paper it is taken to be $V_0 = 10\mathrm{ms}^{-1}$. It should further be noted that $PDF_{wind}dV$ is dimensionless and non-dimensionalizing the AEP it also follows that $PDF_{wind}d\tilde{V}$ is dimensionless. In all of this paper $A\tilde{E}P$ is computed by discretization of the integral and computing the integral with the trapezoidal rule given as $\int_{\tilde{V}_{CI}}^{\tilde{V}_{CO}} f(\tilde{V};C_T,\tilde{R})d\tilde{V} \approx \sum_{i=1}^{N}\frac{f(\tilde{V}_{i+1};C_T,\tilde{R})+f(\tilde{V}_i;C_T,\tilde{R}))}{2}\Delta\tilde{V}_i$ where the discretization (N) was found to become insignificant with $N = 200$.

Baseline rotor

The work here aims at demonstrating improved rotor performance compared to a baseline design. This baseline design is chosen to be a turbine operating at the Betz-limit below rated wind speed and keeping a constant power above rated.

$$C_{T,0} = \frac{8}{9} \approx 0.889, \qquad C_{P,0} = \frac{16}{27} \approx 0.593 \tag{8}$$

This choice of baseline mimics the typical practice of designing wind turbines to target operation with maximum C_P below rated power. In reality, turbines will not achieve maximum C_P at $C_T = 8/9$ since losses alter the relationship between C_T and C_P, but this does not change the fact that turbines are operated at the point of maximum C_P. Figure 2 shows the power and thrust curves for the baseline rotor.

In this paper, all results presented as the change in performance relative to that of the baseline rotor. For this reason , all the relevant variables will be normalized by the corresponding baseline rotor values.

$$\Delta R = \frac{R}{R_0} - 1 \tag{9}$$

$$\Delta\tilde{P} = \frac{C_P R^2}{C_{P,0}R_0^2} - 1 \tag{10}$$

$$\Delta\tilde{L} = \frac{C_T R^{L_{exp}}}{C_{T,0}R_0^{L_{exp}}} - 1 \tag{11}$$

$$\Delta A\tilde{E}P = \frac{A\tilde{E}P}{A\tilde{E}P_0} - 1 \tag{12}$$

where $\tilde{L}$ is a generalized load that will be introduced in the next subsection.

2.2 Scale laws and constraints for Design Driving Loads

In this section, examples of static aerodynamic *Design Driving Loads* (DDL) will be presented. These examples are not meant to be exhaustive, but include several of the key considerations that constrain practical design of wind turbine rotors. From the

https://doi.org/10.5194/wes-2019-28
Preprint. Discussion started: 8 July 2019
© Author(s) 2019. CC BY 4.0 License.

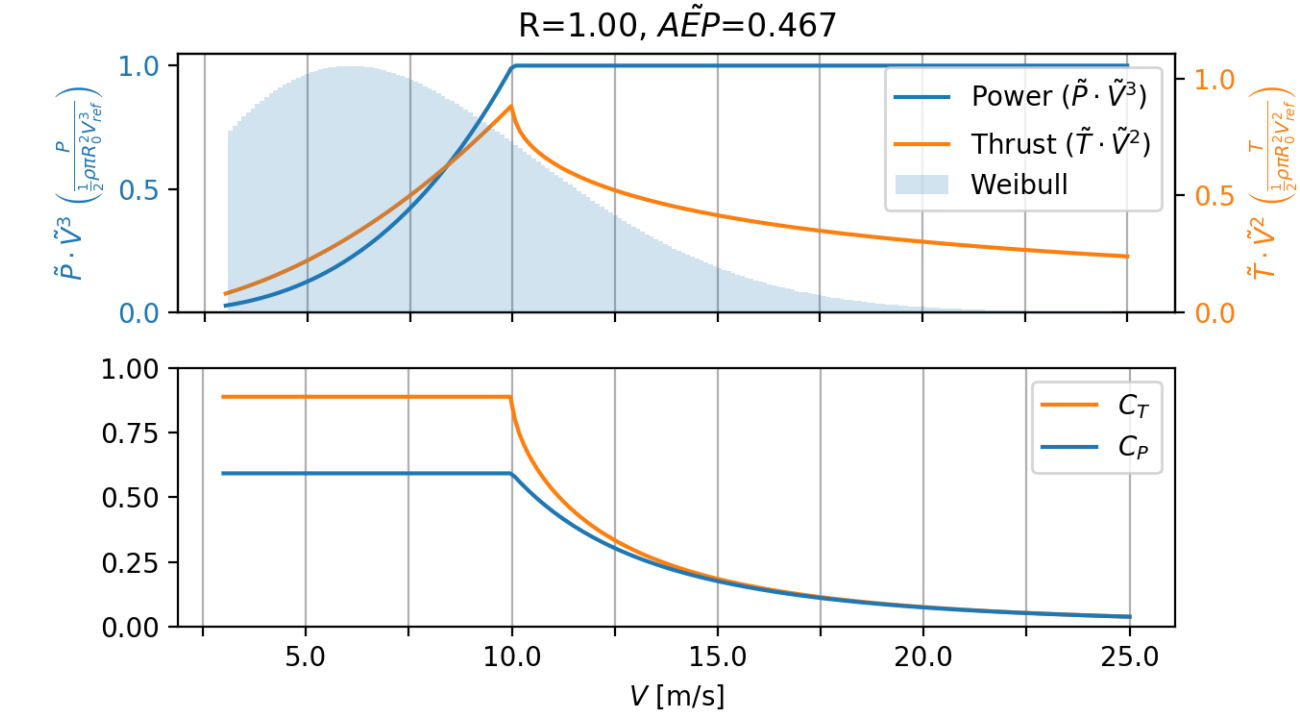

Figure 2. Top: The dimensionless power and thrust for the baseline rotor as a function of wind speed. Overlaid (in blue) the Weibull wind speed frequency distribution used throughout (IEC-class III: $V_{avg} = 7.5$, $k = 2$). Bottom: C_T and C_P as a function of wind speed. These curves reflect how most turbines are operated today, targeting maximum power efficiency below rated power, which leads to a thrust peak just before rated power.

scaled loads, *Design Driving Load Constraints* (DDLC) are introduced, which limit loads so that these do not exceed the levels of the baseline rotor. Based on the DDL examples, it is shown that DDLCs can be elegantly put in a generalized form.

Thrust (T)

Thrust typically does not limit the design of the rotor itself, but more likely is a constraint imposed from the design of tower and/or foundation. The thrust scaling and the associated DDLC is given by:

Scaling DDLC

$$T = \frac{1}{2}\rho V_0^2 \pi R^2 C_T \quad \Longrightarrow \quad \text{DDLC}(T) = \frac{T}{T_0} = \frac{C_T}{C_{T,0}} \left(\frac{R}{R_0}\right)^2 \leq 1 \tag{13}$$

https://doi.org/10.5194/wes-2019-28
Preprint. Discussion started: 8 July 2019
© Author(s) 2019. CC BY 4.0 License.

eawe european academy of wind energy
Open Access WIND ENERGY SCIENCE DISCUSSIONS

Root flap bending moment (M_{flap})

The root flap moment is the bending moment at the rotational center in the axial flow direction. To compute M_{flap}, the 1D-momentum-theory relations for infinitesimal thrust ($\mathrm{d}T$) and moment ($\mathrm{d}M$) are integrated:

$$\mathrm{d}T = \frac{1}{2}\rho V^2 C_T 2\pi r \mathrm{d}r \tag{14}$$

$$\mathrm{d}M_{flap} = r\mathrm{d}T \tag{15}$$

Where r is the radius location of the infinitesimal load ($r \in [0, R]$). The moment scaling and DDLC can therefore be found as:

Scaling DDLC

$$M_{flap} = \int_0^R \mathrm{d}M_{flap} = \frac{1}{3}\rho V_0^2 C_T \pi R^3 \quad \Longrightarrow \quad \mathrm{DDLC}(M_{flap}) = \frac{M_{flap}}{M_{flap,0}} = \frac{C_T}{C_{T,0}}\left(\frac{R}{R_0}\right)^3 \leq 1 \tag{16}$$

As it is seen M_{flap} scales with R^3 so it grow faster than the power, which grows as R^2. M_{flap} is important for the blade design since the flap-wise aerodynamic loads need to be transferred via the blade structure to root of the blade.

Tip deflection (δ_{tip})

Tip deflection is a common DDLC for contemporary utility-scale turbines, where tip clearance between tower and blade may become critical because of relatively long and slender blades. To get an idea for how tip-deflection scales with changes in loading and rotor radius, Euler-Bernoulli Beam Theory (Bauchau and Craig, 2009, p. 189 eq. 5.40) is used. For the problem here it takes the form:

$$\frac{\mathrm{d}^2}{\mathrm{d}r^2} EI \frac{\mathrm{d}^2\delta}{\mathrm{d}r^2} = \frac{\mathrm{d}T}{\mathrm{d}r} = \frac{1}{2}\rho V^2 C_T 2\pi r \tag{17}$$

Where δ is the deflection in the flap-wise direction of the blade at location r. EI is the stiffness of the blade a location r. For modern turbines the stiffness decrease towards the tip of the blade. To get an estimate for the stiffness it is assumed that stiffness follows the size of the chord ($EI \propto c$). The chord is given by the equation in (Sørensen, 2016, p. 68 eq. 5.26) with an approximation for the outer most part of the blade it can be found that $c \propto R/r$ which means that $EI \propto R/r$. An approximate model for EI can be made that have $EI \propto R/r$:

$$EI(r) = \frac{EI_r}{1 + \left(\frac{EI_r}{EI_t} - 1\right)\frac{r}{R}} \tag{18}$$

Where EI_r is the stiffness at the root and EI_t is the stiffness at the tip of the blade. As mentioned above for wind turbines $EI_r > EI_t$.

With the equation for EI equation 17 can be solved by indefinite integration where the integration constants are determined from the following boundary conditions:

$$\underbrace{\delta(r=0) = 0, \quad \frac{\mathrm{d}\delta}{\mathrm{d}r}(r=0) = 0}_{\text{Clamped root}} \qquad \underbrace{\frac{\mathrm{d}^2\delta}{\mathrm{d}r^2}(r=R) = 0, \quad \frac{\mathrm{d}^3\delta}{\mathrm{d}r^3}(r=R) = 0}_{\text{Free tip}} \tag{19}$$

https://doi.org/10.5194/wes-2019-28
Preprint. Discussion started: 8 July 2019
© Author(s) 2019. CC BY 4.0 License.

eawe european academy of wind energy
Open Access WIND ENERGY SCIENCE DISCUSSIONS

The resulting displacement solution looks the following:

$$\delta = \frac{11\pi}{120}\frac{V^2\rho}{EI_r}C_T R^5 \left(\frac{2}{33}\left(\frac{EI_r}{EI_t}-1\right)\tilde{r}^6 + \frac{1}{11}\tilde{r}^5 - \frac{5}{11}\left(\frac{EI_r}{EI_t}-1\right)\tilde{r}^4 + \frac{10}{11}\left(\frac{2}{3}\frac{EI_r}{EI_t}-\frac{5}{3}\right)\tilde{r}^3 + \frac{20}{11}\tilde{r}^2\right) \tag{20}$$

$$= \frac{11\pi}{120}\frac{V^2\rho}{EI_r}C_T R^5 \delta_{shape}\left(\tilde{r}, \frac{EI_r}{EI_t}\right) \tag{21}$$

Where the normalized radius ($\tilde{r} \in [0,1]$) has been introduced so that $r = R \cdot \tilde{r}$. The maximum deflection occurs at the blade tip ($\tilde{r} = 1$), which leads to the following scaling relation and DDLC for tip deflection:

Scaling DDLC

$$\delta_{tip} = \frac{11\pi}{120}\frac{V^2\rho}{EI_r}C_T R^5 \delta_{shape}\left(\tilde{r}=1, \frac{EI_r}{EI_t}\right) \quad \Longrightarrow \quad \text{DDLC}(\delta_{tip}) = \frac{\delta_{tip}}{\delta_{tip,0}} = \frac{C_T}{C_{T,0}}\left(\frac{R}{R_0}\right)^5 \leq 1 \tag{22}$$

Where it implicitly has been assumed that $\frac{EI_r}{EI_t} = \frac{EI_{r,0}}{EI_{t,0}}$ so that δ_{shape} is not changed when R is increased.

Tip deflection with constant mass

The final example of a DDL is also based on tip deflection, but includes a condition to maintain constant mass of the load carrying structure of the blade. To this end the stylized spar-cap layout depicted in figure 3 is assumed. This layout consists of two planks. The stiffness of a spar-cap structure with homogeneous Young's-modulus (E) can be found from the stiffness of a

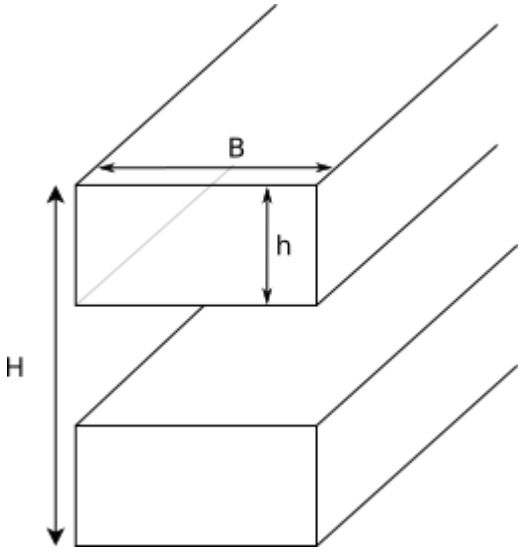

Figure 3. Assumed spar-cap structure with dimensions: H is the total build height, h is the space between planks, and B is the plank width.

https://doi.org/10.5194/wes-2019-28
Preprint. Discussion started: 8 July 2019
© Author(s) 2019. CC BY 4.0 License.

eawe european academy of wind energy
Open Access WIND ENERGY SCIENCE DISCUSSIONS

rectangle and the parallel axis theorem (see figure 3 for variable definition):

$$\left.\begin{array}{c} I_{rect} = \frac{Bh^3}{12} \\ EI = 2E\left(I_{rect} + A\left(\frac{H-h}{2}\right)^2\right) \\ A = Bh \end{array}\right\} EI = 2E\left(\frac{Bh^3}{12} + Bh\left(\frac{H-h}{2}\right)^2\right) = \frac{H^2Bh}{2}\left(\frac{h^2}{3H^2} + \left(1-\frac{h}{H}\right)^2\right) \tag{23}$$

For modern wind turbines $h/H << 1$ meaning that a common approximation is:

$$EI \approx E\frac{H^2Bh}{2} \tag{24}$$

To compute the mass for such a structure it will be assumed that plank height h and the plank width B is constant and that the change in EI comes from a decrease in building height H. If then h is decreased when R is increased the following relationship need to be satisfied in order for the mass of the planks to have constant mass (assuming constant mass density):

$$Rh = R_0h_0 \tag{25}$$

From there it follows that changes in the radius of the rotor will changes the stiffness as:

$$\left.\begin{array}{ll} EI \approx E\frac{H^2Bh}{2} & (24) \\ h = \frac{R_0h_0}{R} & (25) \end{array}\right\} EI \approx E\frac{H^2BR_0h_0}{2R} \tag{26}$$

Combining the equation with the tip deflection equation (21) the following scaling and DDLC can be found:

$$\left.\begin{array}{c} \text{Scaling} \\ \delta_{tip} = \frac{11\pi}{120}\frac{V^2\rho}{EI_r}C_TR^5\delta_{shape}\left(\tilde{r}=1, \frac{EI_r}{EI_t}\right) \\ EI \approx E\frac{H^2BR_0h_0}{2R} \end{array}\right\} \implies \begin{array}{c} \text{DDLC} \\ \text{DDLC}(\delta_{tip+mass}) = \frac{C_T}{C_{T,0}}\frac{EI_{r,0}}{EI_r}\left(\frac{R}{R_0}\right)^5 = \frac{C_T}{C_{T,0}}\left(\frac{R}{R_0}\right)^6 \leq 1 \end{array} \tag{27}$$

Where it has been used that changing h by the same magnitude for the whole blade leads to $\frac{EI_r}{EI_t} = \frac{EI_{r,0}}{EI_{t,0}}$ and hereby not affecting δ_{shape}. It should be noted that by choosing B to change instead will lead to the same scaling, but with the difference being that changing the plank thickness might lead to higher order effects, although they are expected to be insignificant.

Generalizing the constraint form

Considering the four DDLC examples presented above, there appears to be a pattern in the scaling relations that may be written as follows:

$$\frac{C_T}{C_{T,0}}\left(\frac{R}{R_0}\right)^{R_{exp}} \leq 1 \tag{28}$$

https://doi.org/10.5194/wes-2019-28
Preprint. Discussion started: 8 July 2019
© Author(s) 2019. CC BY 4.0 License.

Where R_{exp} is the *DDLC R-Exponent*.

If the constraint limit is met the following relationship can be written as:

$$R = R_0 \left(\frac{C_{T,0}}{C_T} \right)^{\frac{1}{R_{exp}}} \tag{29}$$

3 Formulation of rotor design problems

Based on the performance and constraint relationships outlined in the previous section, this section will present the formulation of rotor design as optimization problems. Two different classes of problems are introduced, namely: *Power Capture optimization* and *AEP optimization*, where the latter is a generalization of the former with the constraint depending on wind speed.

3.1 Power Capture optimization

The optimization problem can be stated as:

$$\underset{C_T, \tilde{R}}{\text{maximize}} \quad \tilde{P} = \frac{1}{2} \left(1 + \sqrt{1 - C_T} \right) C_T \tilde{R}^2 \tag{30}$$

$$\text{subject to} \quad \frac{C_T}{C_{T,0}} \tilde{R}^{R_{exp}} \leq 1 \tag{31}$$

Where the definition of $\tilde{R} = R/R_0$ has been used for consistency . The solution for this optimization problem is presented in the 4.1 section.

It should be noted that this optimization problem is similar to the problem that is given by Chaviaropoulos and Sieros (2014) where they optimize while keeping M_{flap}. So the optimization problem in this paper is a generalization of their optimization problem.

3.2 AEP optimization

In contrast to the above mentioned optimization of power capture, optimization with respect to AEP requires to determine $C_T(\tilde{V})$ so a function opposed to a scalar value. It is also necessary to fix the rated power to a constant value, while the wind speed at which rated power is reached is allowed to change. The problem can be formulated as:

$$\underset{C_T(\tilde{V}), \tilde{R}}{\text{maximize}} \quad A\tilde{E}P = \int_{\tilde{V}_{CI}}^{\tilde{V}_{CO}} \tilde{P}(C_T(\tilde{V}), \tilde{R}) \cdot \tilde{V}^3 \cdot PDF_{wind}(\tilde{V}) d\tilde{V} \tag{32}$$

$$\text{subject to} \quad \begin{aligned} & \tilde{V}^2 \frac{C_T(\tilde{V})}{C_{T,0}} \tilde{R}^{R_{exp}} \leq 1, \quad \text{(DDLC)} \\ & \frac{27}{16} \tilde{P}(C_T(\tilde{V}), \tilde{R}) \tilde{V}^3 \leq 1, \quad \text{(rated power)} \end{aligned} \tag{33}$$

Where the the wind speed scaling has been added to the DDLC.

https://doi.org/10.5194/wes-2019-28
Preprint. Discussion started: 8 July 2019
© Author(s) 2019. CC BY 4.0 License.

eawe european academy of wind energy
Open Access WIND ENERGY SCIENCE DISCUSSIONS

4 Results and discussion

This section discusses the solutions of the rotor design optimization problems introduced in the previous section.

4.1 Optimizing for power capture

The constrained optimization problem to maximize power capture, as stated in the section 3, may be simplified based on the observation that optimum solutions will occur at the DDL constraint limit. To understand this, consider that the power capture of a rotor with an inactive constraint may always be improved by growing the rotor until the constraint is met. This is true irrespective of what DDLC that determines the rotor design. Hence, an explicit relation $\tilde{R}(C_T)$ can be used to reformulate from a constrained optimization problem in two variables to an unconstrained optimization problem in one variable.

$$\left.\begin{aligned} \tilde{P}(C_T,\tilde{R}) &= \frac{1}{2}\left(1+\sqrt{1-C_T}\right)C_T\tilde{R}^2 \quad (5)\\ \tilde{R} &= \left(\frac{C_{T,0}}{C_T}\right)^{\frac{1}{R_{exp}}} \quad (29) \end{aligned}\right\} \implies \tilde{P}\left(C_T\right) = \frac{C_{T,0}^{2\frac{1}{R_{exp}}}}{2}\left(1+\sqrt{1-C_T}\right)C_T^{1-2\frac{1}{R_{exp}}} \tag{34}$$

With the optimization problem now being:

$$\underset{C_T}{\text{maximize}} \quad \tilde{P} = \frac{C_{T,0}^{2\frac{1}{R_{exp}}}}{2}\left(1+\sqrt{1-C_T}\right)C_T^{1-2\frac{1}{R_{exp}}} \tag{35}$$

By differentiating the objective function 34 with respect to C_T and finding its root, the optimal C_T as a function of R_{exp} is arrived at:

$$\frac{d\tilde{P}(C_T)}{dC_T} = 0 \implies \tag{36}$$

$$C_T = \frac{8\left(R_{exp}^2 - 3R_{exp} + 2\right)}{\left(3R_{exp}-4\right)^2} \tag{37}$$

This unique solution is a maximum, which is apparent from the always positive signs of ΔP in figure 4. This figure shows the optimal solution for C_T and C_P, as well as the relative change in radius (ΔR) and power (ΔP) compared to the baseline rotor. From the two left plots, C_P is observed to approach the dashed baseline performance (Betz rotor) much faster than C_T as R_{exp} increases. This is a consequence of the relationship between C_T and C_P (figure 1). Especially around the Betz-limit the gradient is very small, which means that changes in C_T does not lead to proportional changes in C_P. Turning to the two plots on the right in figure 4, it is seen that the lower C_P is more than compensated by increasing R since the relative change in power (ΔP) is always positive.

When maximizing power capture for a given thrust ($R_{exp} = 2$); blue dashed vertical line in figure 4), it is seen that the impractical solution of an infinitely large rotor with low aerodynamic loading results. Alternatively, the maximum power for a given flap root moment ($R_{exp} = 3$; orange line) may be achieved by increasing the rotor radius by 11.6% compared to the baseline design (maximum C_P). The corresponding relative increase in power ΔP is 7.6%. Finally, designs constrained by

https://doi.org/10.5194/wes-2019-28
Preprint. Discussion started: 8 July 2019
© Author(s) 2019. CC BY 4.0 License.

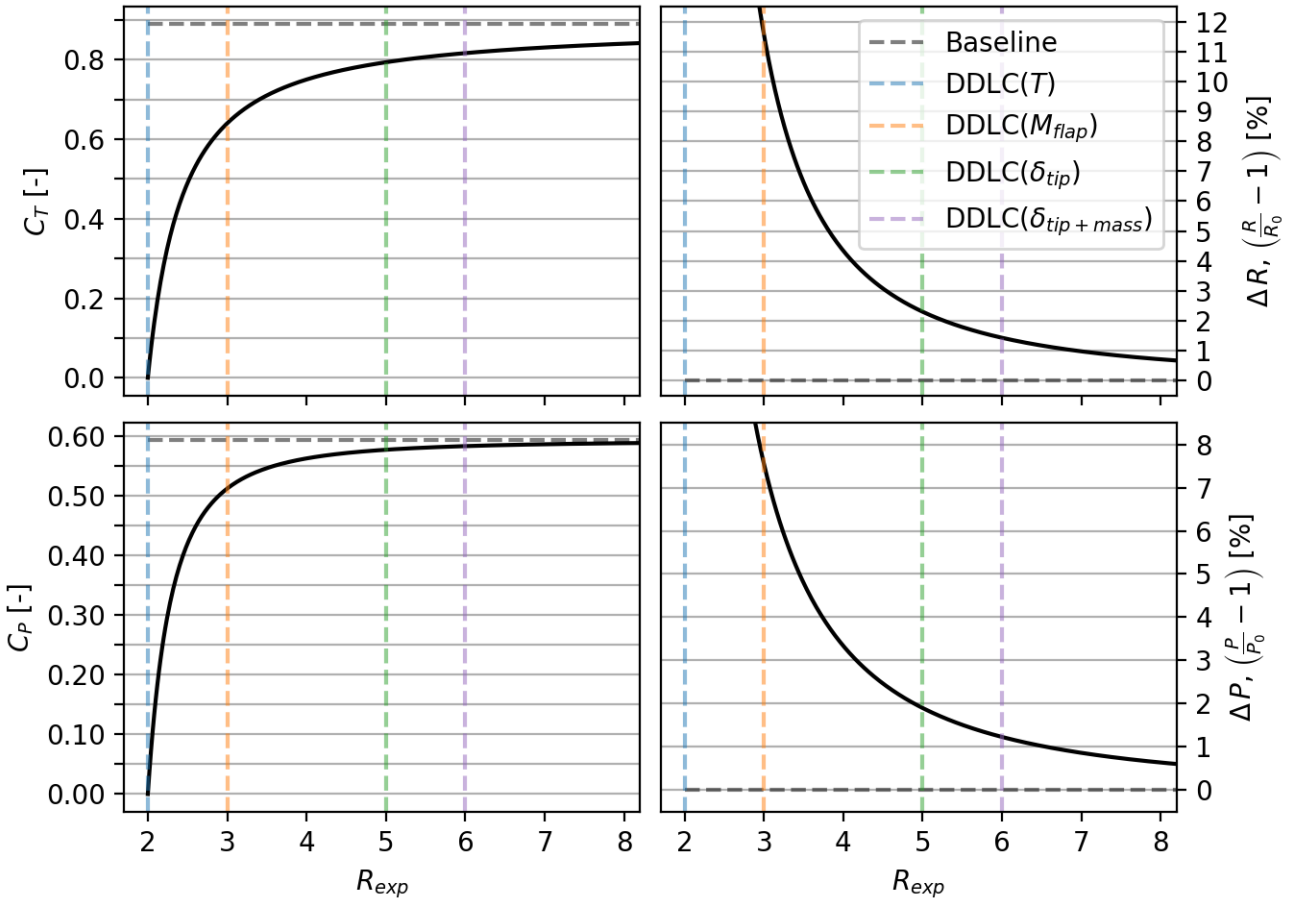

Figure 4. Top left: Optimal C_T as a function of the constraint R-exponent (R_{exp}). Low left: R_{exp} vs. C_P, notice that the optimal C_P curve has a steeper slope and hugs the baseline closer than C_T. Top right: R_{exp} vs. relative change in radius ΔR. Lower right: R_{exp} vs. relative change in power capture ($\Delta\tilde{P}$). Despite the similar shape of curves a difference between the two is that $\Delta P(R_{exp} \to 2) = 50\%$ where $\Delta R(R_{exp} \to 2) \to \infty$. The vertical lines represent each of the example constraints. (**DDLC=Design Driving Load Constraint*).

tip-deflection ($R_{exp} = 5$; green line) allow the relative power ΔP to increase by 1.90% with a relative change in radius ΔR of 2.30%. A table with the results for the the increase in power-capture (ΔP) and radius (ΔR) for 4 designs ($R_{exp} = 2, 3, 5, 6$) can be seen in figure 6. As a conclusion, rotors with an active static aerodynamic DDLC should not be designed for maximum C_P as more power can be generated by rotors with lower C_T and larger radius R, without violating the relevant DDLC. The changes in loading is explained in the next section.

https://doi.org/10.5194/wes-2019-28
Preprint. Discussion started: 8 July 2019
© Author(s) 2019. CC BY 4.0 License.

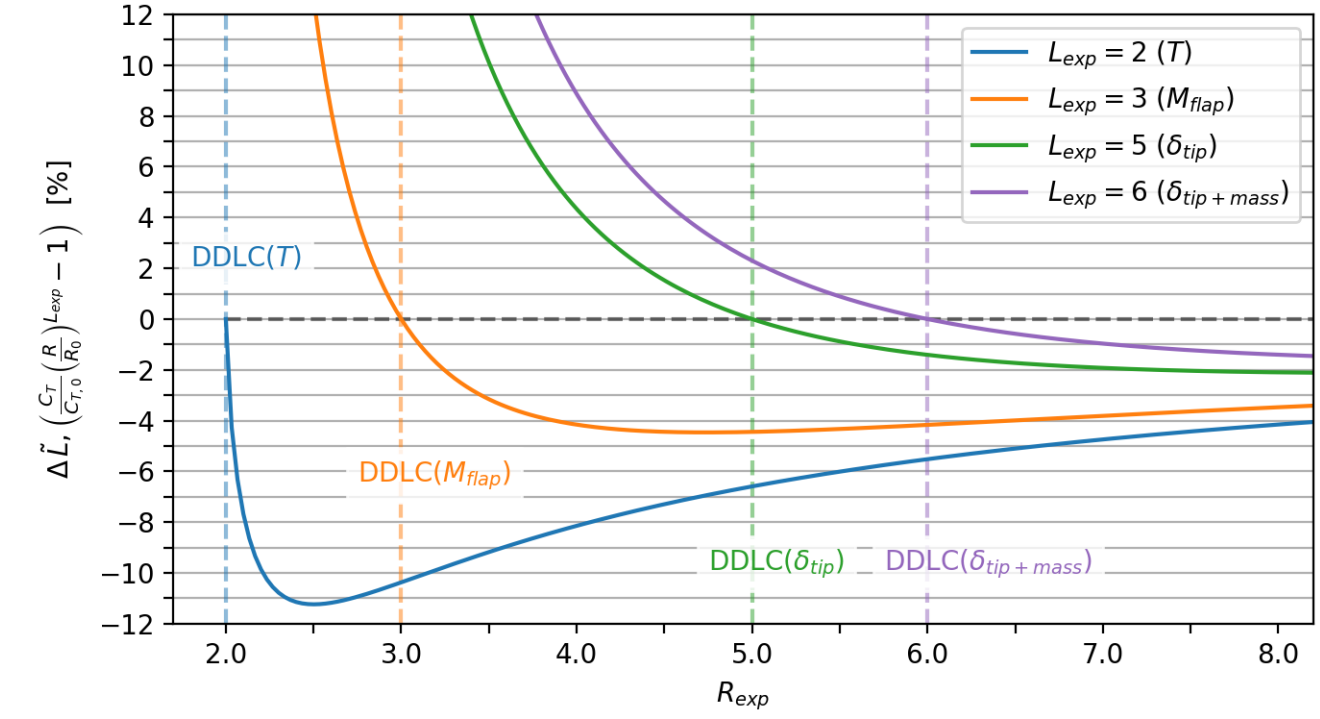

Figure 5. Relative change in different rotor load parameters ($\Delta\tilde{L}$) depending on DDLC. The scaling of loads have the form $\tilde{L} = C_T R^{L_{exp}}$, e.g. $L_{exp} = 2$ scales as the rotor thrust T and $L_{exp} = 5$ scales as the tip deflection δ_{tip}. Each curve depicts how a load parameter would change depending on design driving constraint. As an example consider a design limited by tip deflection DDLC(δ_{tip}), i.e. $R_{exp} = 5$ matching the dashed green line. Tip deflection meets requirements, while thrust (T) is lowered 6.6% and flap moment M_{flap} by 4.4%.

Effect on loads

Even though meeting the constraint limits means that the chosen DDL will be the same as the baseline, it is interesting to know what happens to the loads that scale different than the DDL. As an example, if the DDLC is M_{flap} ($R_{exp} = 3$) it is given that it will not change relative to the baseline, but it could be interesting to know what happens to the T and δ_{tip}.

To investigate it we will introduce a *Generalized Load* (L) as a measure of how loads scale.

$$L = K_0 V_0^2 C_T R^{L_{exp}} \tag{38}$$

Where K_0 is a scaling constant and L_{exp} is the *Generalized Load Exponent*. The Generalized Load equation can be made non-dimensional as:

$$\tilde{L} = \frac{L}{K_0 V_0^2 R_0^{L_{exp}}} = C_T \tilde{R}^{L_{exp}} \tag{39}$$

https://doi.org/10.5194/wes-2019-28
Preprint. Discussion started: 8 July 2019
© Author(s) 2019. CC BY 4.0 License.

eawe european academy of wind energy
Open Access WIND ENERGY SCIENCE DISCUSSIONS

The difference between L_{exp} and R_{exp} is that R_{exp} results in a design, wheres L_{exp} is a load for a design. As an example take a design made for tip-deflection ($R_{exp} = 5$) then $L_{exp} = 3$ will describe the M_{flap} load for that design.
An equation for the relative change $\Delta\tilde{L}$ can be found in terms of the baseline rotor as:

$$\left.\begin{aligned} \tilde{L} &= C_T \tilde{R}^{L_{exp}} \quad (39) \\ \tilde{R} &= \left(\frac{C_{T,0}}{C_T}\right)^{\frac{1}{R_{exp}}} \quad (29) \\ \tilde{L}_0 &= C_{T,0}\tilde{R}_0^{L_{exp}} = C_{T,0} \end{aligned}\right\} \implies \Delta\tilde{L} = \frac{\tilde{L}}{\tilde{L}_0} - 1 = \left(\frac{C_T}{C_{T,0}}\right)^{1-\frac{L_{exp}}{R_{exp}}} - 1 \tag{40}$$

Since it is known that $C_T \leq C_{T,0}$ the following can be concluded:

$L_{exp} < R_{exp}$	The load is lower than the baseline level
$L_{exp} = R_{exp}$	The load is identical to the baseline level
$L_{exp} > R_{exp}$	The load is larger than the baseline level

This agrees with figure 5, which illustrates the effect of design constraints (DDLC) on different loads. For example, consider tip-deflection ($R_{exp} = 5$, DDLC(δ_{tip}), dashed green line). Looking at the green solid line ($L_{exp} = 5$) it is seen that the relative change in L is zero as expected. Now looking at the loads with $L_{exp} < R_{exp}$, namely thrust ($L_{exp} = 2$) and flap-moment ($L_{exp} = 3$) it is seen that ΔL is lower than the baseline with $\Delta T = -6.6\%$ and $\Delta M_{flap} = -4.4\%$. But the loads where $L_{exp} > R_{exp}$ the loads are increased. If there was a load that scaled like $L_{exp} = 6$ the load would be increased by $\Delta L_{(L_{exp}=8)} = +2.3\%$. Furthermore, figure 5 shows that the relative decrease in load is always most pronounced for the thrust ($L_{exp} = 2$), the biggest impact occurring around $R_{exp} \approx 2.5$. All the relative change curves have distinct minima, but at the same time are characterized by large plateaus of relatively small change. Another observation is how quickly the curves grows for $L_{exp} > R_{exp}$. As an example take DDLC(M_{flap}) in this case $\Delta\delta_{tip} = +24.5\%$ and $\Delta L_{(L_{exp}=6)} = +38.9\%$. The relative change in loads becomes smaller as R_{exp} increases. A sketch with a zoomed view of the tip and a table with the values can be seen in figure 6.

https://doi.org/10.5194/wes-2019-28
Preprint. Discussion started: 8 July 2019
© Author(s) 2019. CC BY 4.0 License.

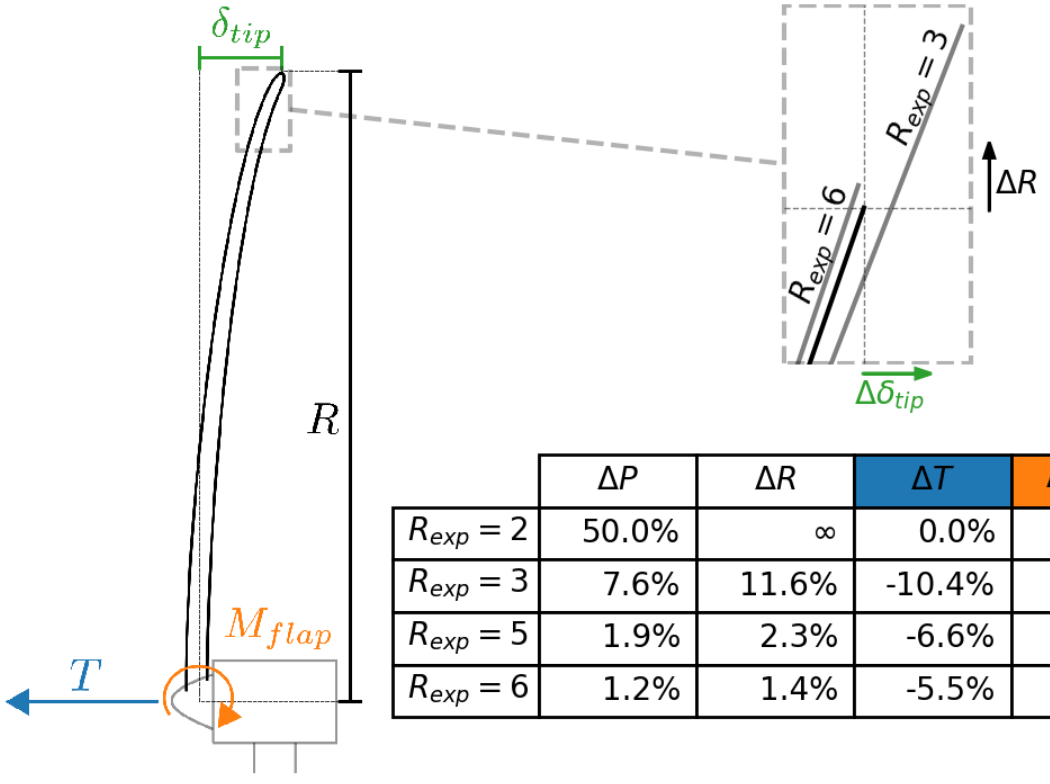

	ΔP	ΔR	ΔT	ΔM_{flap}	$\Delta\delta_{tip}$
$R_{exp} = 2$	50.0%	∞	0.0%	∞	∞
$R_{exp} = 3$	7.6%	11.6%	-10.4%	0.0%	24.5%
$R_{exp} = 5$	1.9%	2.3%	-6.6%	-4.4%	0.0%
$R_{exp} = 6$	1.2%	1.4%	-5.5%	-4.2%	-1.4%

Figure 6. Sketch of a turbine with the load/structural response outlined. The zoomed figure shows the radius increase (ΔR) and the change in tip-deflection ($\Delta\delta_{tip}$) for two different DDLCs (bold black line is the baseline). The table shows the relative change in power, radius and load/structural response for different DDLCs. $R_{exp} = 2$ is a thrust constraint design, $R_{exp} = 5$ is a tip-deflection constraint design.

https://doi.org/10.5194/wes-2019-28
Preprint. Discussion started: 8 July 2019
© Author(s) 2019. CC BY 4.0 License.

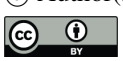

eawe european academy of wind energy
Open Access WIND ENERGY SCIENCE DISCUSSIONS

4.2 Low induction rotor

The concept was mentioned in the introduction since it has had some attention over the recent years. The Low Induction Rotors (LIR) are rotors designed with lower axial induction a than the level that maximizes C_P. The concept is to a certain degree analogous with optimization of rotors with respect to power-capture. Using the value for C_T from power-capture optimization will not give the a design that will reach the constraint limit, since the increase in rotor radius will make the turbine reach rated power earlier than the baseline. An additional optimization is therefore required where R is increase until the constraint limit is reached. The LIR is illustrated by the examples in figure 7 and 8 where the present design framework has been applied with constraints pertaining to respectively flap moments ($R_{exp} = 3$) and tip deflections ($R_{exp} = 5$).

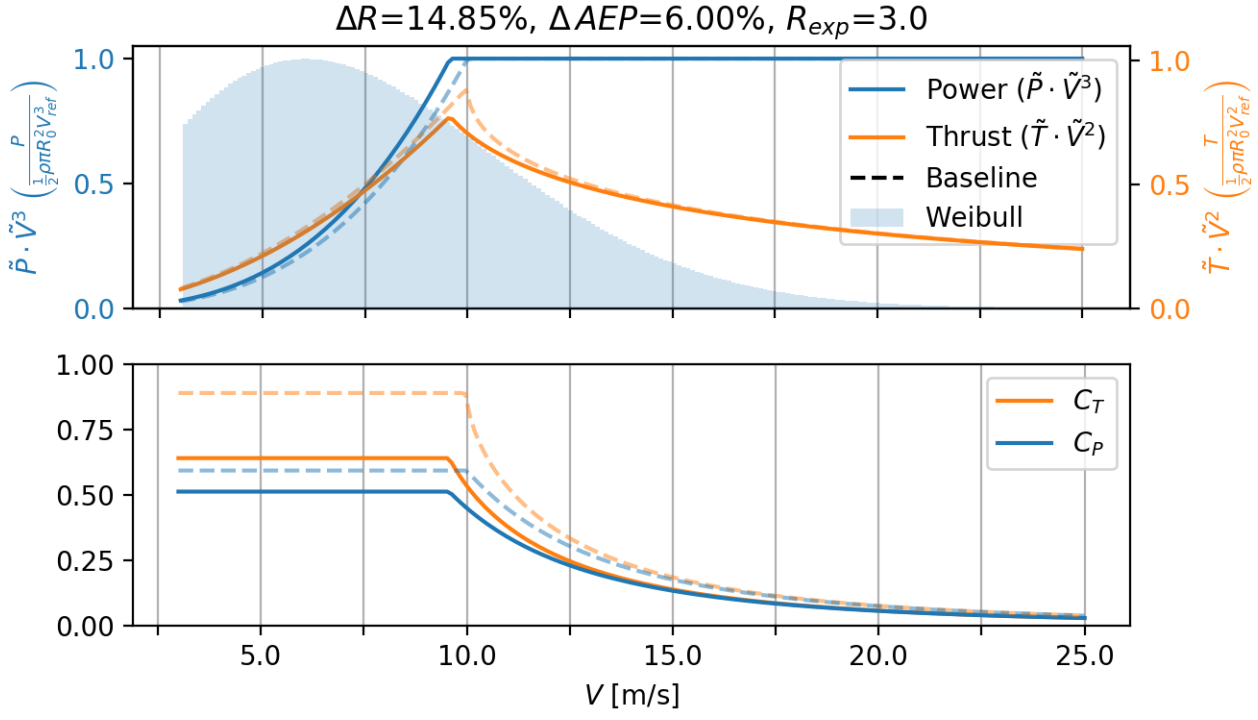

Figure 7. Power and thrust curves for low induction rotor, designed using present method with DDLC exponent $R_{exp} = 3$, which corresponds to a M_{flap} constraint.

In both cases the resulting power curves are slightly above the equivalent baseline ones, and the thrust peaks are reduced compared with the baseline. The relative change in AEP results in a smaller change than the change in power at the design point. For the case with DDLC(M_{flap}), $\Delta AEP = 6.0\%$ while the power capture increased by $\Delta P = 7.6\%$. The corresponding improvements for a tip deflection constrained rotor (DDLC(δ_{tip})) are $\Delta AEP = 1.1\%$ and $\Delta P = 1.9\%$. The lower relative improvement for the LIR is related to the amount of the power that is produced below rated power. The results for LIR is

https://doi.org/10.5194/wes-2019-28
Preprint. Discussion started: 8 July 2019
© Author(s) 2019. CC BY 4.0 License.

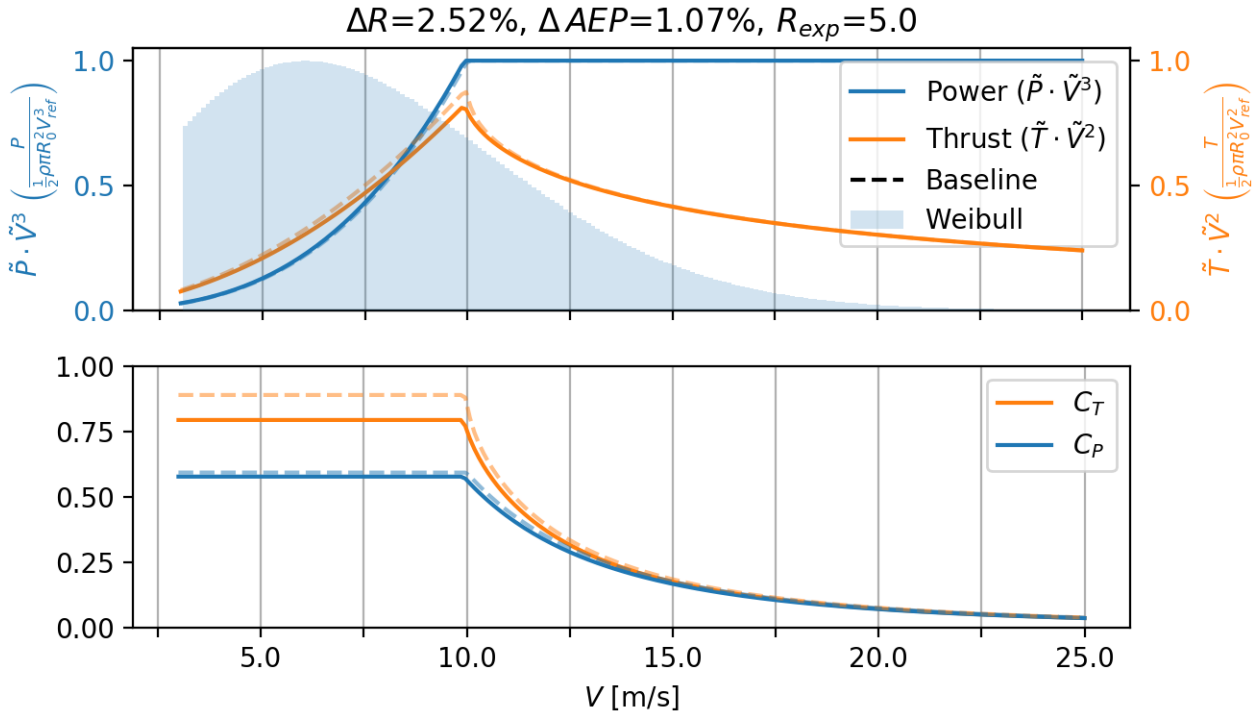

Figure 8. Power and thrust curves for rotor with DDLC exponent $R_{exp} = 5$, corresponding to a δ_{tip} constraint.

summarized in figure 9 with a table and a sketch showing the relative changes in AEP, radius, thrust, root-flap-moment and tip-deflection for 4 different designs ($R_{exp} = 2, 3, 5, 6$).

https://doi.org/10.5194/wes-2019-28
Preprint. Discussion started: 8 July 2019
© Author(s) 2019. CC BY 4.0 License.

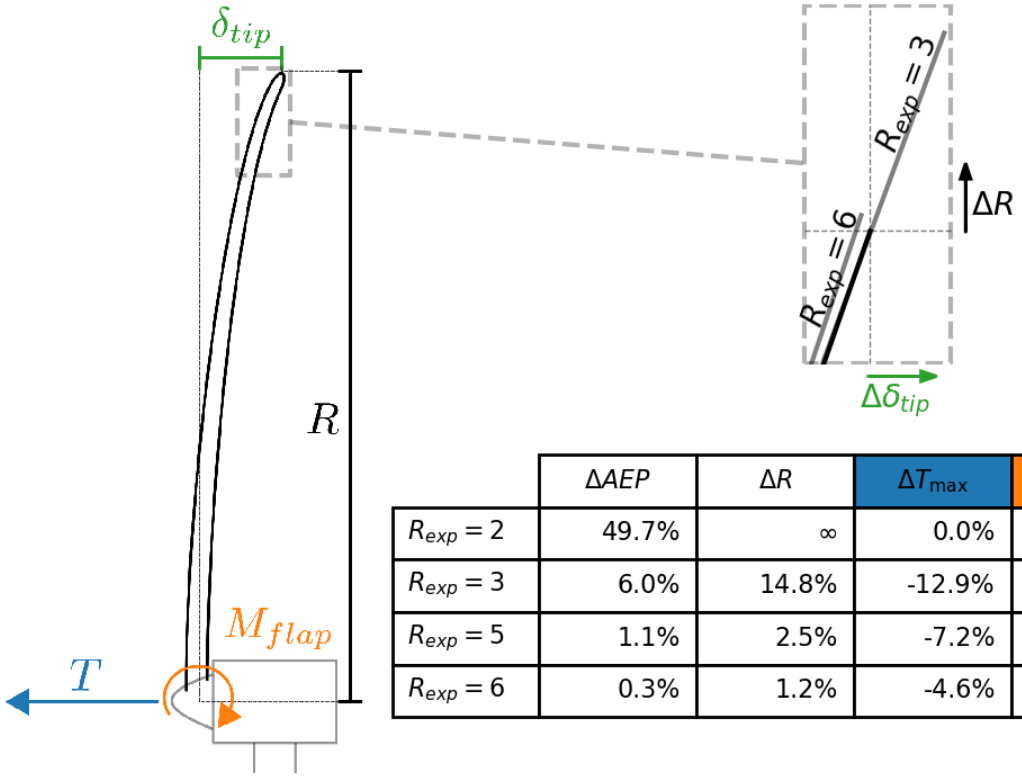

	ΔAEP	ΔR	ΔT_{max}	$\Delta M_{flap,max}$	$\Delta\delta_{tip,max}$
$R_{exp} = 2$	49.7%	∞	0.0%	∞	∞
$R_{exp} = 3$	6.0%	14.8%	-12.9%	0.0%	31.9%
$R_{exp} = 5$	1.1%	2.5%	-7.2%	-4.9%	0.0%
$R_{exp} = 6$	0.3%	1.2%	-4.6%	-3.5%	-1.2%

Figure 9. Sketch of a turbine with the load/structural response outlined. The zoomed figure shows the radius increase (ΔR) and the change in tip-deflection ($\Delta\delta_{tip}$) for two different DDLCs (bold black line is the baseline). The table shows the relative change in power, radius and load/structural response for different DDLCs. $R_{exp} = 2$ is a thrust constraint design, $R_{exp} = 5$ is a tip-deflection constraint design.

https://doi.org/10.5194/wes-2019-28
Preprint. Discussion started: 8 July 2019
© Author(s) 2019. CC BY 4.0 License.

eawe european academy of wind energy
Open Access WIND ENERGY SCIENCE DISCUSSIONS

4.3 AEP optimized rotor

As mentioned in section 3, the variables considered for optimization of AEP are $C_T(\tilde{V})$ as well as $\tilde{R}$. In this formulation, C_T can be adjusted independently for each wind speed, which ideally can be achieved through blade pitch control. The relative radius $\tilde{R}$ couples the rotor operation across all wind speeds, as it necessarily is constant. Based on initial studies, the optimizer targets solutions with three distinct operational ranges, which ordered by wind speed are:

- Operation with maximum power efficiency ($\max C_P$)
- Operation at constraint limit (constant thrust T)
- Operation at rated power

this can be used to make C_T a function of $\tilde{R}$ hereby decreasing the optimization problem to an unconstrained optimization in one variable ($\tilde{R}$). The C_T function is given as:

$$C_T(\tilde{V},\tilde{R}) = \begin{cases} \frac{8}{9} & \frac{8}{9} \leq \tilde{V}^{-2} C_{T,0} \tilde{R}^{-R_{exp}}, \quad (\max C_P) \\ \tilde{V}^{-2} C_{T,0} \tilde{R}^{-R_{exp}} & 1 \leq \frac{27}{16}\frac{1}{2}\left(1+\sqrt{1-C_T}\right) C_T \tilde{R}^2 \tilde{V}^3, \quad \text{(constraint limit)} \\ 1 = \frac{27}{16}\frac{1}{2}\left(1+\sqrt{1-C_T}\right) C_T \tilde{R}^2 \tilde{V}^3 & 1 > \frac{27}{16}\frac{1}{2}\left(1+\sqrt{1-C_T}\right) C_T \tilde{R}^2 \tilde{V}^3, \quad \text{(rated power)} \end{cases} \tag{41}$$

Where the last equation needs to be solved to get C_T, the solution is a third-order polynomial, which is easier solved numerically.

The only free parameter that need to be determined to find the optimal AEP is $\tilde{R}$. The optimization problem can therefore be reformulated as:

$$\underset{\tilde{R}}{\text{maximize}} \quad A\tilde{E}P = \int_{\tilde{V}_{CI}}^{\tilde{V}_{CO}} \tilde{P}(C_T(\tilde{V},\tilde{R}),\tilde{R}) \cdot \tilde{V}^3 \cdot PDF_{wind}(\tilde{V}) d\tilde{V} \tag{42}$$

The problem can be solved with most optimization solvers since the AEP can be computed explicitly if $\tilde{R}$ is given. The optimization problem was solved with the L-BFGS-B algorithm described in Zhu et al. (1997) though the use of Scipy (Millman and Aivazis (2011)).

Examples of the resultant power and thrust curves can be seen in figure 10 and 11, for DDLC(M_{flap}) and DDLC(δ_{tip}) respectively. Looking at figure 10 ($R_{exp} = 3$) it is clear that the power and thrust curves has changed quite substantially, compared to the baseline Betz-rotor (dashed curves). The thrust curve do not have a sharp peak any more, but a flat plateau. This is often refereed to as thrust-clipping, peak-shaving or force-capping. It comes from the DDLC equation 41 which shows that $C_T \propto \tilde{V}^{-2}$, and since thrust is proportional to $T \propto C_T \tilde{V}^2$ it means that the thrust is constant. As mentioned the region where the rotor is thrust-cliped is also where the DDLC is active, so opposed to the baseline and LIR rotor the DDLC is active over a larger range of V. The larger range of V is also part of why $\Delta R = 44.6\%$ which is a huge increase. As a result it also leads to a large increase in $\Delta AEP = 19.9\%$. This is a very large change in $\tilde{R}$ and the feasibility of such a design is doubtful. As it is shown later the change in maximum loads (see figure 13) shows a significant change in loads with $L_{exp} > R_{exp}$.

https://doi.org/10.5194/wes-2019-28
Preprint. Discussion started: 8 July 2019
© Author(s) 2019. CC BY 4.0 License.

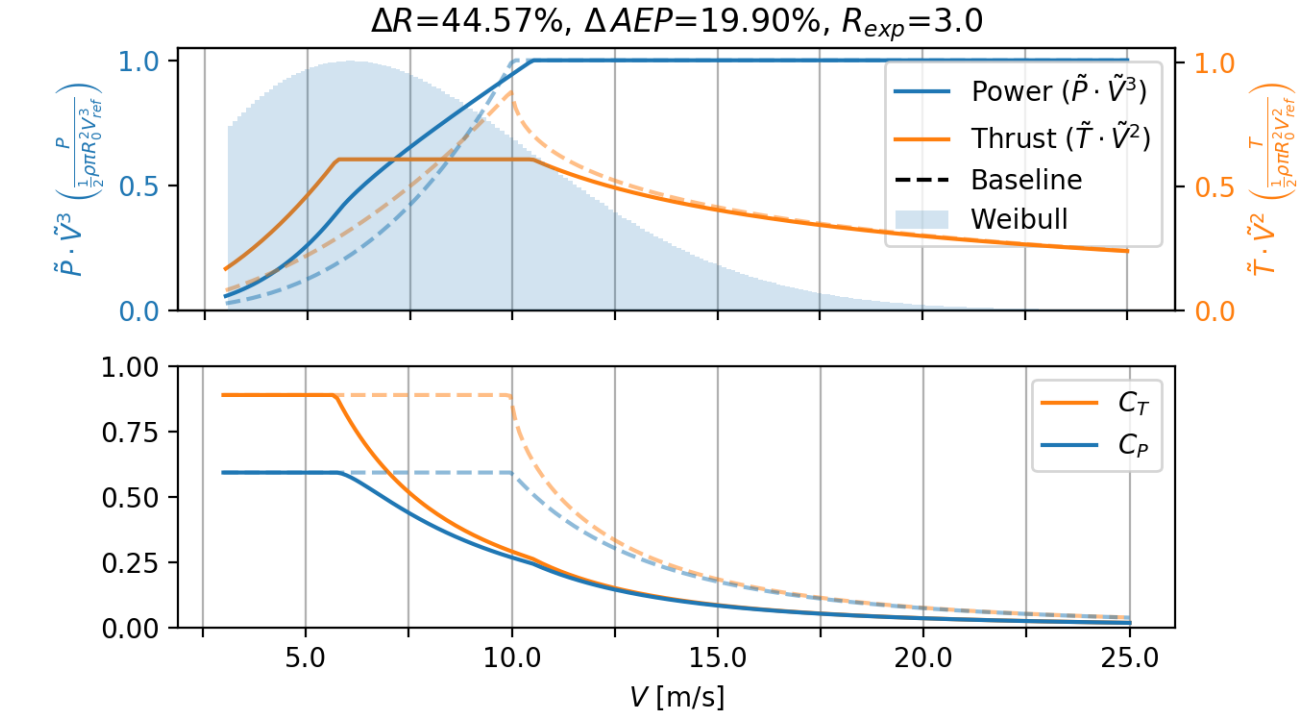

Figure 10. Power and thrust curve for AEP optimized rotor with DDLC exponent is $R_{exp} = 3$ which is equivalent to a constraint on M_{flap}.

A more realistic design for modern turbines is found in figure 11 ($R_{exp} = 5$). Here the changes is less but still significant with $\Delta R = 10.7\%$ and $\Delta AEP = 5.8\%$. It shows the same shape with the thrust-cliped curve, but now it is over a smaller range of V. Thrust-clipping is also found by Buck and Garvey (2015a) to be a beneficial way to lower CoE.

In figure 12 the relative change in R and AEP can be see as a function of the DDLC R-exponent. The plot both contains the result for the AEP-optimized rotor (AEP opt., solid black line) and for the Low Induction Rotor (Low ind. dash-dotted gray line). The difference between the two is significant especially for ΔAEP. A thing to notes is that in both cases ΔR grows to infinity as R_{exp} goes toward 2. But for ΔAEP it will go towards a finite value. The results for the AEP optimized rotor is summarized in figure 14 with a table and a sketch, that shows the relative changes in radius. The loads are explained in the next section.

Effect on loads

In figure 13 a plot of the relative change in maximum loads as a function of the DDLC R-exponent. The relative max load ($\Delta\tilde{L}_{\max}$) is not comparing the loads at each $\tilde{V}$ but the max load for the baseline at $\tilde{V} = 1$ to the max load for the optimized rotor for any $\tilde{V}$. The plot in figure 13 is similar to the plot in figure 5 with the difference being that it is for the AEP-optimized rotor and Power-Capture optimized rotor respectively. Comparing the two plots, the range for the y-scale in the two plots should be

https://doi.org/10.5194/wes-2019-28
Preprint. Discussion started: 8 July 2019
© Author(s) 2019. CC BY 4.0 License.

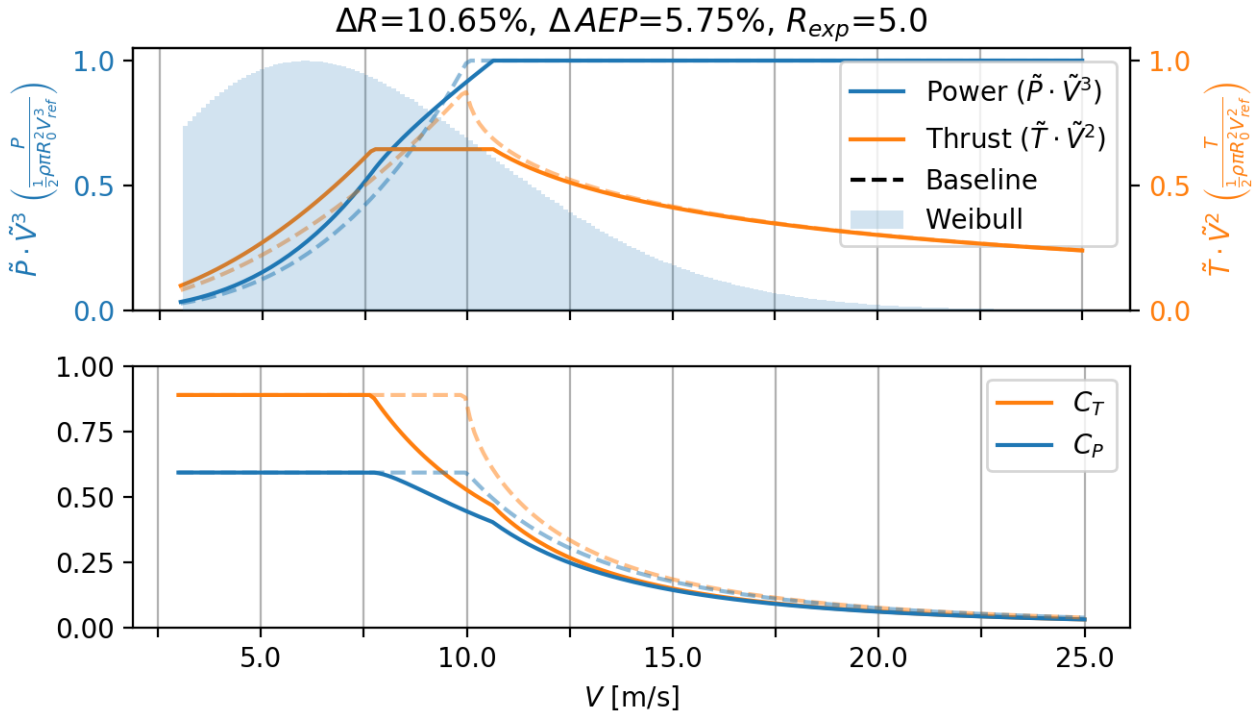

Figure 11. Power and thrust curve for AEP optimized rotor with DDLC exponent is $R_{exp} = 5$ which is equivalent to a constraint on δ_{tip}.

noted with figure 13 having the larger range. It also means that the relative change in the loads for the AEP-optimized rotor experiencing a larger relative change. But it also has the consequence that loads with $L_{exp} > R_{exp}$ grows faster especially for larger values of R_{exp} (> 5). A summary for the AEP optimized rotor can be seen in figure 14, where a table for 4 different design ($R_{exp} = 2, 3, 5, 6$) shows the relative change in AEP, radius, thrust, root-flap-moment and tip-deflection.

https://doi.org/10.5194/wes-2019-28
Preprint. Discussion started: 8 July 2019
© Author(s) 2019. CC BY 4.0 License.

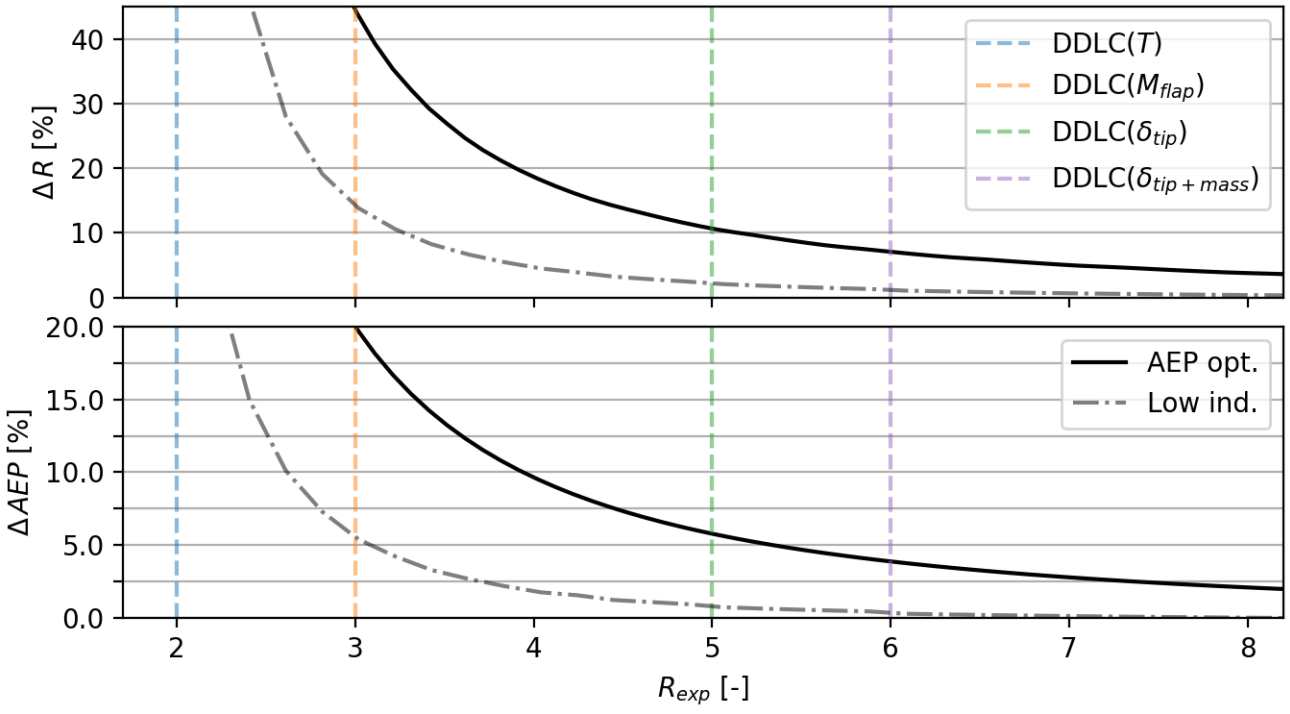

Figure 12. DDLC exponent (R_{exp}) vs. relative change in radius (upper graph, ΔR) and relative change in AEP (lower graph, $\Delta \tilde{AEP}$). The plot both contains the changes for the case for Low Induction (Low Ind., black dashed-dot) and the AEP optimized (AEP opt., black solid). The changes in both AEP and radius is much larger for the AEP optimized rotor. It should be noted that in both cases ΔAEP has a finite value as $R_{exp} \rightarrow 2$, but ΔR is approaching infinity.

https://doi.org/10.5194/wes-2019-28
Preprint. Discussion started: 8 July 2019
© Author(s) 2019. CC BY 4.0 License.

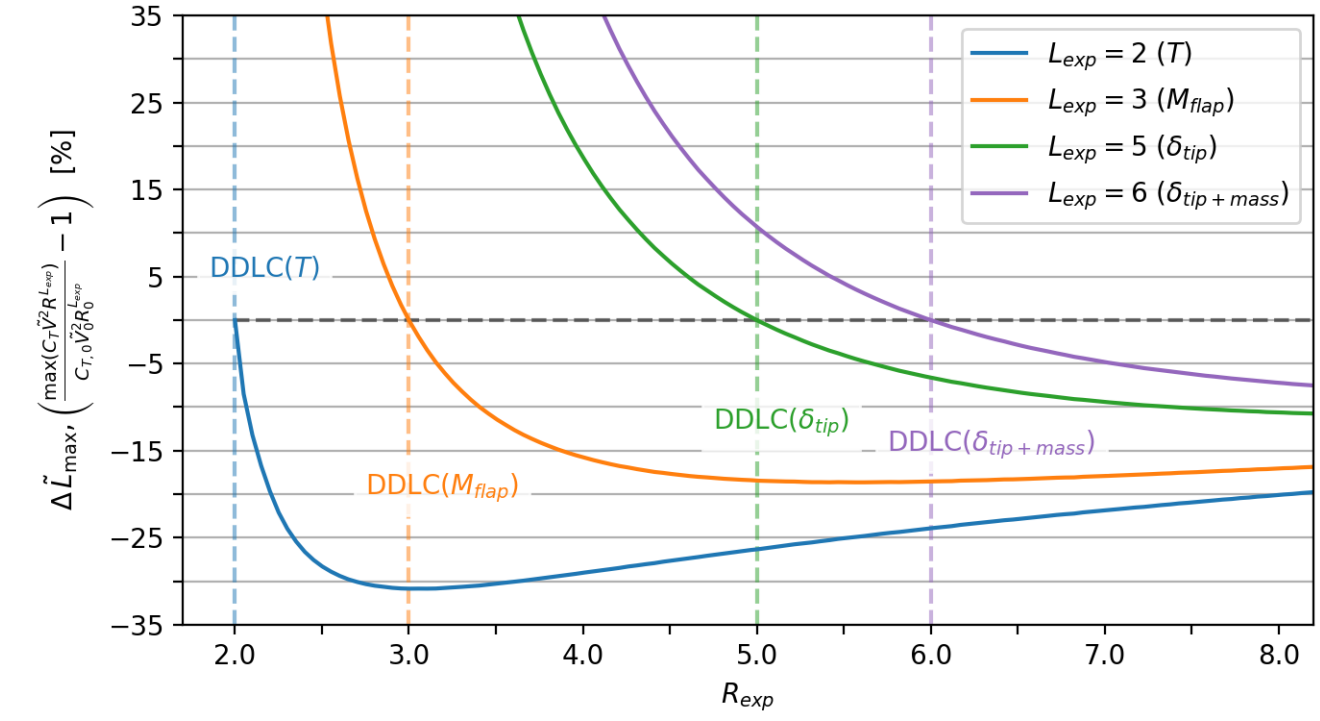

Figure 13. DDLC R-exponent (R_{exp}) vs. relative maximum load ($\Delta\tilde{L}_{\max}$). It is a similar plot to figure 5 but here it is for the AEP-optimized rotor and it is the change in the max load. The range for the y-scale is much larger it this plot than for the power-capture optimized rotor. The potential reduction is therefore more, but it comes with the consequence that $L_{exp} > R_{exp}$ grows faster even for high values of R_{exp}

https://doi.org/10.5194/wes-2019-28
Preprint. Discussion started: 8 July 2019
© Author(s) 2019. CC BY 4.0 License.

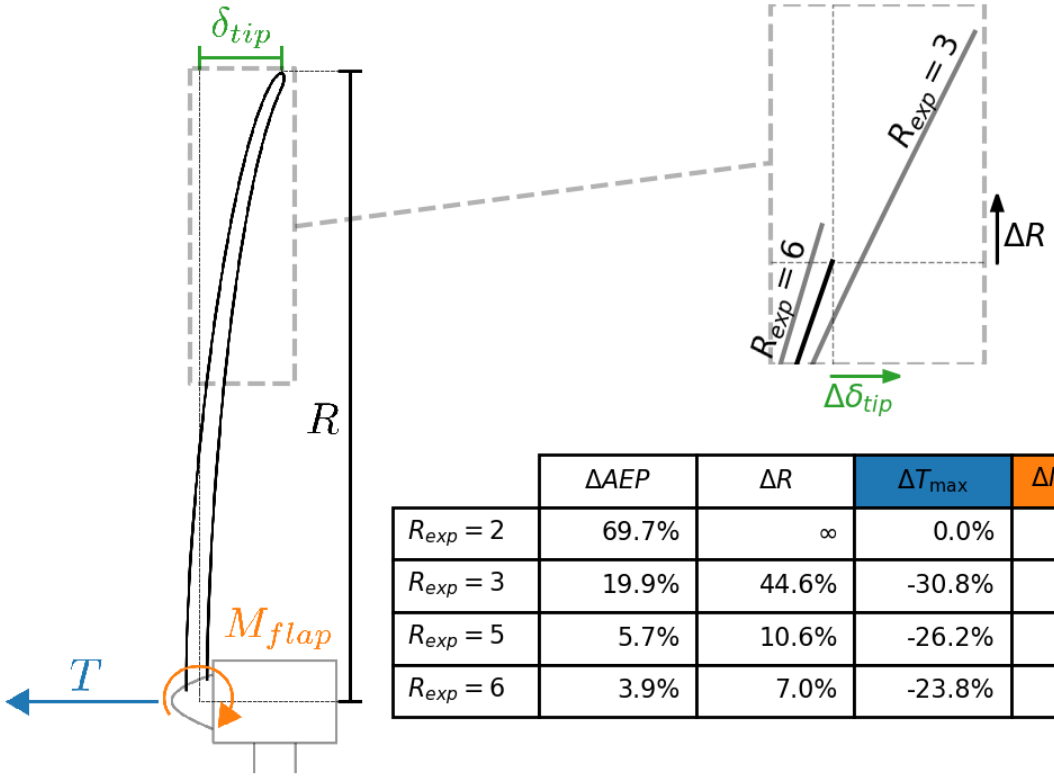

	ΔAEP	ΔR	ΔT_{max}	$\Delta M_{flap,max}$	$\Delta\delta_{tip,max}$
$R_{exp} = 2$	69.7%	∞	0.0%	∞	∞
$R_{exp} = 3$	19.9%	44.6%	-30.8%	0.0%	109.0%
$R_{exp} = 5$	5.7%	10.6%	-26.2%	-18.3%	0.0%
$R_{exp} = 6$	3.9%	7.0%	-23.8%	-18.4%	-6.6%

Figure 14. Sketch of a turbine with the load/structural response outlined. The zoomed figure shows the radius increase (ΔR) and the change in tip-deflection ($\Delta\delta_{tip}$) for two different DDLCs (bold black line is the baseline). The table shows the relative change in power, radius and load/structural response for different DDLCs. $R_{exp} = 2$ is a thrust constraint design, $R_{exp} = 5$ is a tip-deflection constraint design.

https://doi.org/10.5194/wes-2019-28
Preprint. Discussion started: 8 July 2019
© Author(s) 2019. CC BY 4.0 License.

eawe european academy of wind energy
Open Access WIND ENERGY SCIENCE DISCUSSIONS

4.4 Summary of Findings

In table 1 the tables shown in the figures 6,9 and 14 is summarized. It compares the different optimization's to each other.

Opt. PC	ΔP	ΔR	$\Delta T_{(L_{exp}=2)}$	$\Delta M_{flap_{(L_{exp}=3)}}$	$\Delta \delta_{tip_{(L_{exp}=5)}}$
R_{exp}=2	50.0%	∞	0.0%	∞	∞
R_{exp}=3	7.6%	11.6%	-10.4%	0.0%	24.5%
R_{exp}=5	1.9%	2.3%	-6.6%	-4.4%	0.0%
R_{exp}=6	1.2%	1.4%	-5.5%	-4.2%	-1.4%
Opt. LIR	ΔAEP	ΔR	$\Delta T_{(L_{exp}=2)}$	$\Delta M_{flap_{(L_{exp}=3)}}$	$\Delta \delta_{tip_{(L_{exp}=5)}}$
R_{exp}=2	49.7%	∞	0.0%	∞	∞
R_{exp}=3	6.0%	14.8%	-12.9%	0.0%	31.9%
R_{exp}=5	1.1%	2.5%	-7.2%	-4.9%	0.0%
R_{exp}=6	0.3%	1.2%	-4.6%	-3.5%	-1.2%
Opt. AEP	ΔAEP	ΔR	$\Delta T_{(L_{exp}=2)}$	$\Delta M_{flap_{(L_{exp}=3)}}$	$\Delta \delta_{tip_{(L_{exp}=5)}}$
R_{exp}=2	69.7%	∞	0.0%	∞	∞
R_{exp}=3	19.9%	44.6%	-30.8%	0.0%	109.0%
R_{exp}=5	5.7%	10.6%	-26.2%	-18.3%	0.0%
R_{exp}=6	3.9%	7.0%	-23.8%	-18.4%	-6.6%

Table 1. Overview of the optimization results from optimizing Power-Capture (Opt. PC), Low-Induction-Rotor (Opt. LIR) and Annual Energy Production (Opt. AEP)

https://doi.org/10.5194/wes-2019-28
Preprint. Discussion started: 8 July 2019
© Author(s) 2019. CC BY 4.0 License.

eawe european academy of wind energy
Open Access WIND ENERGY SCIENCE DISCUSSIONS

4.5 Limitation of the study and possible improvements

The study shows that for a rotor constraint by a static aerodynamic DDL there is a benefit in lowering the loading and increasing the rotor size in terms of power/AEP. But as it was found by Bottasso et al. (2015) having a rotor with the same load constraint and increasing the radius does not mean that the cost is the same or that it is cost optimal. They found that the increase in AEP did not compensate for the added cost by increasing the rotor radius. This problem of the cost benefit is not directly addressed in this paper, but by the DDLC $\delta_{tip+mass}$ a constraint where the mass is kept constant. It is thought to be a better approximation for a rotor with a fixed price - but this assumption needs to be tested.

Another issue that is not taken into account in this study is the influence of the turbines "self weight". As it was found by Sieros et al. (2012) the self weight becomes more important for larger rotors. In order to accommodate for the added mass a penalty could be added which should scale as $\tilde{R}$ or $\tilde{R}^3$ for "top head mass" and "static blade mass moment" respectively. As discussed above there could also be implemented constraint that will keep the mass or the mass moment. Again this is a limitation of the study.

The fidelity of the models is also a limitation. Even though 1D-aerodynamic-momentum theory is a common approximation to do for first order studies in rotor design it is well known that the constantly loaded rotor is not possible to realize and when losses are included the constant loaded rotor is not the optimal solution any more. At the same time if it was possible to decrease the load at the tip more than at the root it would lead to less tip-deflection than a constant loaded rotor with a similar C_T. Extending the model to be able to handle radial load distribution is one way of detailing the model that could lead to even larger improvements. It could be done through the use of Blade Element Momentum (BEM) theory.

For modern turbine design it is often the case that the structural design is determined by the aero-elastic extreme loads, and with the simplicity of the models in this study this is not taken into consideration. But if the extreme load happens in normal operation it is likely that there is a direct relationship between the steady- and extreme loads, meaning that a decrease in steady loads will also will lead to a decrease in the extreme load. This is an assumption that should be tested in future work.

5 Conclusions

A first order model framework for the design of wind turbine rotors was developed based on aerodynamic 1D-momentum theory and Euler-Bernoulli-Beam theory. This framework introduces the concept of *Design Driving Load* (DDL) for which a generalized form has been developed where loads only differ by a scaling exponent R_{exp}, e.g. thrust scales as $R_{exp} = 2$, root-flap-moment as $R_{exp} = 3$ and tip-deflection as $R_{exp} = 5$. Despite the simplicity of the model, this study has shown important trends in how to design rotors for maximum power capture. It has been shown that the potential increase in power capture is very dependent on the relevant constraint, e.g. whether thrust is the constraining load or the more restrictive tip-deflection. Furthermore, it was concluded that the best way to design a rotor for increased power capture using aero-elastic considerations is not to maximize C_P, but rather to relax C_P and operate at lower loading (lower C_T). How much one should relax C_P depends on the chosen design driving constraint (R_{exp}). The results for optimizing for power capture are summarized in Table 1 (Opt. PC).

https://doi.org/10.5194/wes-2019-28
Preprint. Discussion started: 8 July 2019
© Author(s) 2019. CC BY 4.0 License.

eawe european academy of wind energy
Open Access WIND ENERGY SCIENCE DISCUSSIONS

The optimization of power capture determines the best possible design based on a given wind speed. By considering the *Annual Energy Production* (AEP), an optimal design across the range of operational wind speeds can be found for a given wind speed frequency distribution. Optimal AEP was considered with two different approaches, namely *Low Induction Rotor* (LIR) and full AEP-optimization. For LIR, the C_T value below rated power was set to the value found from power-capture optimization with respect to the chosen R_{exp}. Then the radius was increased to maximize AEP while observing the constraint limit. A summary of results can be seen in Table 1 (Opt. LIR).

For the full AEP-optimization, C_T was allowed to take on any positive value below the Betz limit ($0 \leq C_T \leq 8/9$) for all wind speeds. The optimal AEP is obtained for a rotor that operates in three distinct operational regimes:

- Operation with maximum power efficiency ($\max C_P$)
- Operation at constraint limit (constant thrust T)
- Operation at rated power

The results from the optimization are summarized in Table 1 (Opt. AEP). It shows significantly larger relative improvements in power/energy compared to power-capture and LIR optimized rotors. This comes at the cost of a larger increase in rotor radius. In the range where the optimum turbine operates at the constraint limit, the thrust curve is clipped (also known as peak shaving or force-capping). This is a control feature used for many contemporary turbines, so it is interesting that this study, independently of this knowledge, shows that thrust-clipping is a very efficient way to increase energy capture while observing certain load constraints. It is also the main reason behind the relatively large possible improvements in AEP, as the constraint limit is met over a larger range of wind speeds.

In spite of relatively crude model assumptions made, this paper provides profound insight into the trends of rotor design for maximum power/energy, e.g. the use of thrust clipping. As wind turbine rotors continue develop towards larger diameters with slender (more flexible) blades, the type of design driving load constraints also evolves. With the present model framework, the conceptual implications of this development become clearer where an increase in AEP of up to 5.7% is possible compared to a traditional C_P optimized rotor - without changing technology, using bend-twist coupling or other advanced features. Finally, this work has demonstrated an approach to formulate an optimization objective that couples power and load/structural response though the power-capture optimization. This approach may be extended into less crude model frameworks, e.g. by introducing radial variations in rotor loading.

https://doi.org/10.5194/wes-2019-28
Preprint. Discussion started: 8 July 2019
© Author(s) 2019. CC BY 4.0 License.

eawe european academy of wind energy
Open Access WIND ENERGY SCIENCE DISCUSSIONS

Author contributions. KL came up with the concept and main idea, as well as made the analysis. All author have interpreted the results and made suggestions for improvements. KL prepared the paper with revisions of all co-authors.

Competing interests. The authors declare that they have no conflict of interest.

Acknowledgements. We would like to thank Innovation Fund Denmark for funding the industrial PhD project which this article is a part of.
400 We would like to thank all employees at Suzlon Blade Sciences Center for being a great source of motivation with their interest in the results.

We would like to thank all people at DTU Risø who came with valuable inputs.

https://doi.org/10.5194/wes-2019-28
Preprint. Discussion started: 8 July 2019
© Author(s) 2019. CC BY 4.0 License.

eawe european academy of wind energy
Open Access WIND ENERGY SCIENCE DISCUSSIONS

References

Bauchau, O. and Craig, J.: Structural Analysis, https://doi.org/10.1007/978-90-481-2516-6, 2009.

Bottasso, C. L., Croce, A., and Sartori, L.: Free-form Design of Low Induction Rotors, in: 33rd Wind Energy Symposium, https://doi.org/10.2514/6.2015-0488, 2015.

Buck, J. A. and Garvey, S. D.: Analysis of Force-Capping for Large Wind Turbine Rotors, Wind Engineering, 39, 213–228, https://doi.org/10.1260/0309-524X.39.2.213, 2015a.

Buck, J. A. and Garvey, S. D.: Redefining the design objectives of large offshore wind turbine rotors, Wind Energy, 18, 835–850, https://doi.org/10.1002/we.1733, 2015b.

Chaviaropoulos, P. K. and Sieros, G.: Design of Low Induction Rotors for use in large offshore wind farms, Ewea 2014, pp. 51–55, 2014.

Fleming, P. A., Ning, A., Gebraad, P. M. O., and Dykes, K.: Wind plant system engineering through optimization of layout and yaw control, Wind Energy, 19, 329–344, https://doi.org/10.1002/we.1836, 2016.

Kelley, C. L.: Optimal Low-Induction Rotor Design, in: Wind Energy Science Conference 2017, 2017.

Millman, K. J. and Aivazis, M.: Python for scientists and engineers, Computing in Science and Engineering, 13, 9–12, https://doi.org/10.1109/MCSE.2011.36, 2011.

Perez-Moreno, S. S., Zaaijer, M. B., Bottasso, C. L., Dykes, K., Merz, K. O., Réthoré, P. E., and Zahle, F.: Roadmap to the multidisciplinary design analysis and optimisation of wind energy systems, Journal of Physics: Conference Series, 753, https://doi.org/10.1088/1742-6596/753/6/062011, 2016.

Sieros, G., Chaviaropoulos, P., Sørensen, J. D., Bulder, B. H., and Jamieson, P.: Upscaling wind turbines: theoretical and practical aspects and their impact on the cost of energy, Wind Energy, 15, 3–17, https://doi.org/10.1002/we.527, 2012.

Sørensen, J. N.: The general momentum theory, vol. 4, https://doi.org/10.1007/978-3-319-22114-4_4, 2016.

Zahle, F., Tibaldi, C., Verelst, D. R., Bitche, R., and Bak, C.: Aero-Elastic Optimization of a 10 MW Wind Turbine, https://doi.org/10.2514/6.2015-0491, 2015.

Zhu, C., Byrd, R. H., Lu, P., and Nocedal, J.: Algorithm 778: L-BFGS-B: Fortran subroutines for large-scale bound-constrained optimization, ACM Transactions on Mathematical Software, 23, 550–560, https://doi.org/10.1145/279232.279236, 1997.